Design of a self-stable and population-controllable co-culture system in E. coli and its applications

Hao Chen
Institute of Microbiology, Chinese Academy of Sciences https://orcid.org/0000-0002-8885-8663
Qun Liu
Institute of Microbiology, Chinese Academy of Sciences
Xuanlin wang
Institute of Microbiology, Chinese Academy of Sciences
Weifeng Liu
State Key Laboratory of Microbial Resources & CAS Key Laboratory of Microbial Physiological and Metabolic Engineering, Institute of Microbiology, Chinese Academy of Sciences
Shuang-Yan Tang
CAS Key Laboratory of Microbial Physiological and Metabolic Engineering, State Key Laboratory of Microbial Resources, Institute of Microbiology, Chinese Academy of Sciences, Beijing, China.
Shizhong Li
Institute of Microbiology, Chinese Academy of Sciences
Baixue Lin
Institute of Microbiology, Chinese Academy of Sciences
Yong Tao (taoyong@im.ac.cn)
Institute of Microbiology, Chinese Academy of Sciences https://orcid.org/0000-0003-3106-6953

Article

Keywords:

Posted Date: March 16th, 2022

DOI: https://doi.org/10.21203/rs.3.rs-1429863/v1

Abstract

Modular co-culture engineering has been applied to divide labor among different strains in the biomanufacturer of substances through complicated metabolic pathways. However, dynamic instability, uncontrollable population ratios, and lack of mathematical models have hindered its further application. In this study, we built a mathematical model and used it to design a self-stable co-culture system with adjustable population ratios of two engineered *Escherichia coli* strains. As an indicator product, the yield of chlorogenic acid was successfully increased by 16.5% by adjusting the population ratio in the system. This system provides a robust and scalable production platform for modular co-culture engineering.

The co-culture system was confirmed to be a symbiotic system with high carbon atom economy for acetyl-CoA-derived chemicals by optimization of poly-β-hydroxybutyrate production, which was 2.82-fold higher than it was for wild-type *E. coli*. The conversion rate of glucose to poly-β-hydroxybutyrate also was 3.19-fold higher in the co-culture system. Our results provide new insights into possible future applications of co-culture systems.

1. Introduction

Traditional metabolic engineering using axenic cultures has provided great opportunities for the production of many valuable compounds[1,2]; however, bottlenecks in the construction of relatively complex metabolic pathways[3–7] have hindered its wider application. They include excessive metabolic pressure of a single strain[8], interferences in the process of metabolic pathway optimization[9], and imbalance of competitive metabolic pathways[10]. To overcome these obstacles, modular co-culture engineering, which is realized by co-culture of multiple strains, is considered to be a smart solution and has been studied extensively. A complex metabolic pathway is divided into different modules that become the responsibility of different strains. Therefore, modular co-culture engineering can reduce the metabolic burden of individual strains, offer the flexibility to balance the biosynthetic strength between pathway modules, reduce the undesired interference of different pathway modules, and plug-and-play modules for the biosynthesis of different target products[4].

Modular co-culture engineering is an emerging field that has some challenges, including how to maintain the stability of and how to adjust the population ratio, as well as the lack of analytical and predictable mathematical models.

Maintaining the stability of the strain population ratio can be difficult[3–7]. Despite this, many remarkable achievements using modular co-cultivation engineering have been reported[11–17]. These studies showed the advantages of modularity, but the population ratio did not maintain long-term balance, and each strain grew relatively independently because there was no growth-related relationship among the co-cultured strains. Competition among co-cultured members for substrates results in a highly dynamic population composition. Such populations are difficult to replicate steadily and are not conducive to further optimization, and therefore are unsuitable for large scale applications.

To maintain a relatively balanced population ratio, a number of different methods have been used. For example, different strains that synergistically ingested complex carbon sources were co-cultured[18,19]. However, the utilization of degraded carbon sources is often competitive. Co-culture of strains that exclusively use different carbon sources can avoid competition to a certain extent[20,21], but in such a population there is no interdependent relationship among members, and therefore it lacks the spontaneous stability of population ratio. Quorum sensing can be used to automatically maintain population ratio stability in a certain range[22–24]; however, the cell density will be limited because quorum sensing is based on the response to cell density, rather than on relative proportions in a co-culture[25,26]. Establishing cross-feeding has also been widely used to stabilize the population proportion through the interaction of metabolites[27–34], and this method has had some positive effects in maintaining the stability of population ratios. However, the deeper issues of which type of cross-feeding is better at maintaining a stable proportion, and how to select appropriate interactive metabolites to maintain the balance of population ratio, have not yet been reported.

The key to the optimization of inter-module strength is how to adjust the population proportion to a desired value[3–7]. Most studies have focused on the initial population ratio, but the inevitable overgrowth of dominant strains within the system[15] and failure to change the final population ratio because of the inherent stability of the symbiosis[35] are still challenges in co-culture systems.

Analytical and predictable mathematical models are urgently required to provide general principles for the establishment of stable co-culture systems and for the rational design of modular co-culture engineering platforms[3–7, 36,37].

In this study, we aimed to build a universally applicable production platform for modular co-culture engineering with population ratio self-stability, adjustability, predictability, and scalability. We constructed a mathematical model to analyze the population structure in high cell density cultivation of three types of dual-strain co-culture modes. Key factors that were needed to maintain the equilibrium state of the population ratio and the ratio value determinants were deduced using the model.

A self-stable and population-adjustable *Escherichia coli* co-culture system was successfully designed (Fig. 1). It was a unidirectional cross-feeding co-culture system composed of an α-ketoglutaric acid (AKG) donor strain (DS) and an AKG acceptor strain (AS), which we called the DS-AS co-culture system. To measure the performance of the system, the chlorogenic acid (CGA) synthesis pathway was divided into two modules and implanted into the DS-AS co-culture system. The yield of the indicator product CGA in a bioreactor was increased by 16.5% by adjusting the population ratio, which verified the applicability of the co-culture system.

This symbiotic DS-AS co-culture system has attractive overall metabolic characteristics that result in high carbon atom economy for acetyl-CoA-derived chemicals, as was shown by the optimization of poly-β-hydroxybutyrate (PHB) yield and conversion rate of glucose to PHB. These findings provide new insights into the application of DS-AS co-culture systems.

2. Results

2.1 Establishing a mathematical model of cross-feeding co-culture system

Mathematical models of independent growth, and unidirectional and bidirectional cross-feeding co-culture systems were established based on the Monod equation. Then, the factors necessary for a stable population ratio were investigated.

To achieve a stable population ratio, the same specific growth rate of the two strains should be guaranteed (see Eqs. S32–S34 in Supplementary Information). For the independent growth model, forming a stable population ratio is difficult unless $\mu_{m1}=\mu_{m2}$ because the proportion of the strain with a larger μ_m will approach 100% with culture time (Fig. 2A3).

The unidirectional cross-feeding model has self-stability of population ratio when $\mu_{m1}<\mu_{m2}$ (see Eq. S37 in Supplementary Information, Fig. 2B3). The equilibrium ratio (ER) for population can be represented as $ER=\frac{X_1}{X_2}=\frac{1}{Y_{H1}K_{H1}}$ (where X is the biomass, Y_{H1} is the biomass yield coefficient on H1, and K_{H1} is the generation coefficient of H1; see Eqs. S38–S42 in Supplementary Information for details), which implies the ER is determined by only the product of two constants. This relationship indicates the robustness to the maximum specific growth rate and initial population ratio of the two strains. No obvious accumulation of interactive substance H1 was found at the ER (Fig. 2B4). If $\mu_{m1}>\mu_{m2}$, the donor strain will overgrow the acceptor strain, resulting in an unbalanced population ratio (Fig. 2B3).

In the bidirectional cross-feeding model, the two strains are donor and acceptor to each other. Only the interactive substance H1 provided by the strain with relatively low μ_m was able to stabilize the population ratio, which is not substantially different from unidirectional cross-feeding. The ER can be represented by: $\frac{X_1}{X_2}=\frac{1}{K_{H1}Y_{X2/H1}}$, where Strain1 has a lower μ_m (see Eq. S50 in Supplementary Information). The other interactive substance H2 will accumulate in the environment, which is not conducive to high cell density growth (Fig. 2C4, C5). Furthermore, each yield coefficient must meet $K_{H1}Y_{X2/H1}K_{H2}Y_{X1/H2}>1$; otherwise, the material circulation of the co-culture system will be interrupted, and the growth of each strain will stop (see Eqs. S51–S54 in Supplementary Information).

The unidirectional cross-feeding model was therefore shown to be more suitable than the bidirectional cross-feeding model for constructing a stable population ratio because it was easy to design and no obvious accumulation of interactive metabolites was found.

2.2 Design of a unidirectional cross-feeding co-culture system in *E. coli*

We applied the mathematical model to design a unidirectional cross-feeding co-culture system with AKG as the interactive substance with two *E. coli* strains each with a central carbon metabolic pathway modification (Fig. 1A). The AKG DS with *sucA* knocked-out and the AKG AS with *icd* knocked-out carried constitutively expressed mCherry and GFP, respectively. The fluorescent proteins were used to help determine the numbers of the two strains.

The DS cannot express 2-ketoglutarate dehydrogenase and tends to accumulate AKG due to downstream blocking. Thus, succinyl-CoA, which is an important precursor for cell growth[38], can only be produced by a reverse tricarboxylic acid (TCA) cycle rather than the forward TCA cycle, which results in a low specific growth rate[39]. Overaccumulation of AKG in the environment can cause growth inhibition[40], and therefore the DS could hardly grow when cultured independently.

The AS has no isocitrate-homoisocitrate dehydrogenase activity and therefore cannot synthesize AKG, which is also an important precursor for cell growth[38]. As a result, the AS cannot grow independently with glucose as the sole carbon source unless supplemented with exogenous AKG. We assumed that when the DS and AS were co-cultured, the AS could grow by absorbing the AKG secreted by the DS, thereby eliminating the growth inhibition caused by excessive AKG accumulation. (Indeed, both AKG and AKG-derivatives such as glutamate can be released by the DS as interactive substances and absorbed by the AS. To simplify the description of our results, AKG and AKG-derivatives were treated as AKG without distinction because the abundance of AKG and AKG-derivatives would form a dynamic balance catalyzed by bidirectional enzymes in cells.)

To illustrate the symbiotic relationship between the two strains, non-contact spreading tests were performed on solid medium. The growth of the two strains increasingly improved as the two strains came closer to each other. On the far side, the DS showed weak growth and the AS hardly grew (Fig. 3A, B). This finding suggests that the DS formed a symbiont relationship with the AS by extracellular metabolite exchange without physical contact.

At shaker scale, the DS and AS could hardly grow independently when cultured overnight in chemically defined medium supplemented with 10 g/L glucose, whereas the co-culture groups grew well regardless of the inoculation ratio (Fig. 3C).

When cultured in the modified inorganic medium independently in a batch bioreactor, the AS barely grew and the growth rate of the DS gradually decreased with the final OD = 5 with the 20 g/L glucose exhausted (Fig. 3D). The DS-AS co-culture system grew exponentially and the OD_{600} was 21.1 when the glucose was exhausted. The experiments at different scales showed that symbiosis occurred in the DS-AS co-culture system, and this relationship ensured that the two strains could coexist stably.

2.3 Stability test of population ratio in a batch bioreactor

The experimental data of different initial population ratios are consistent with the predictions (Fig. 4A–D). (The mathematical model of the DS-AS co-cultivation system is described in section 3 of

Supplementary Information.) The OD_{600} was > 120 (Fig. 4A, B) and the proportion of the DS gradually approached 20% and remained stable regardless of the inoculation ratio (Fig. 4C-D), indicating that the co-culture system was self-stable in population ratio and was robust to proportion fluctuations. The trend of the results predicted by the model was highly consistent with the experimental results, which further confirmed the good predictability accuracy of the model.

2.4 Population ratio control

To precisely control the population ratio to desired values, we set about changing one of the two yield coefficients—K_{H1} and Y_{H1}—that determined the ER derived from the model. For the DS, succinyl-CoA, which can be synthesized from succinic acid (SCA), is a limiting factor that affects growth. When supplemented with SCA, the utilization rate of AKG by the DS increases because of the demand for cell growth, which reduces the exocytosis of AKG, thereby reducing the K_{H1} value and increasing the population ratio of the DS. For the AS, AKG is one of the factors that limits growth rate. When AKG is supplemented in the environment artificially, more of the AS can be grown, thus increasing the population ratio of the AS.

In the fed-batch bioreactor, AKG or SCA was supplemented into the feeding medium containing 60% glucose. The OD_{600} of each experimental group was not affected by the addition of these substances (Fig. 4E). Supplementation with 3% AKG decreased the proportion of the DS from 19.8–6.9% and supplementation with 3% SCA increased the proportion of the DS to 31.9% (Fig. 4F). After adjustment, the DS:AS population ratios remained stable with the growth of strains. These results confirmed that the ER was successfully controlled by exogenous inputs of AKG or SCA under the premise of self-stability. Although the population ratio of the DS is currently adjustable from 6.9–31.9%, when applied to modular co-culture metabolic engineering, combinations of strains and modules can be interchanged to increase the proportion range.

2.5 Modular co-culture engineering for CGA production

To test the applicability of the DS-AS co-culture system in modular co-culture engineering, we selected the biosynthesis of CGA as an example. Caffeic acid (CA) de novo synthesis (CA pathway) and CGA conversion from CA (CGA pathway) are relative independent[12]. We integrated the CA and CGA pathways into the DS-AS co-culture system to form CA and CGA modules with exogeneous quinic acid supplementation, which was expected to reduce the accumulation of toxic intermediate CA and increase the content of the final product CGA by balancing the proportion between modules (Fig. 5A).

The CA and CGA pathways were implanted into the DS and AS, respectively, to form two combinations. The proportion of CA modules in combination 1 tended to reach 36.7% (Fig. 5B), whereas the proportion of CA modules in combination 2 remained above 95% (Fig. 5C). In combinations 1 and 2, 0.65 mM and 0.02 mM CGA were obtained, respectively, and 1.6 mM CA was detected in both combinations. In the two combinations, the ratio of the two strains stabilized to a relatively fixed range, indicating that the co-culture system stabilized the proportion of different modules and uncontrolled overgrowth of one module

was avoided. The accumulation of CA indicates that the CA module needs to be down-regulated to obtain higher CGA concentrations.

To achieve higher CGA production and a lower CA proportion, the proportion of each module was tuned by the population ratio control described in section 2.4. Increasing of the proportion of CGA modules improved CGA production (Fig. 6D) and reduced CA accumulation (Fig. 6C), indicating that the lack of the CGA module may be the limiting factor in CGA synthesis. CGA yield was significantly increased ($P < 0.05$) in 6% AKG group (0.813 mM in 84 h) compared with its yield in the control group (0.698 mM in 84 h). The ratio of CGA to CA was 1.20 in the 6% AKG group, indicating an increase of 154% compared with the ratio in the control (0.473). These results indicate that the ratio of CA and CGA modules was successfully optimized to enhance CGA production with the co-culture system, which verified the applicability of the DS-AS co-culture system in modular co-culture engineering.

2.6 Economical carbon efficiency of the DS-AS co-culture system for PHB production

In the DS-AS co-culture system, the overall TCA cycle flux is relatively low because of the interruption of the TCA cycle, and therefore some cellular intermediates, such as acetyl-CoA (Ac-CoA), may be more easily accumulated. This characteristic can be used to facilitate the enhanced production of corresponding chemicals and reduce inefficient carbon burning caused by the TCA cycle.

The abundance of Ac-CoA, citric acid, cis-aconitic acid, isocitric acid, phenylpyruvate, and other substances in the DS-AS co-culture system was analyzed by metabolomics and was found to be significantly ($P < 0.05$) higher than their abundance in the control group (Fig. 7A). In particular, the abundance of Ac-CoA in the DS-AS co-culture system was 25 times higher than that in the control group, and this feature was used to boost PHB production (Fig. 7B).

Plasmid pRB1s-CAB carrying the PHB synthesis genes was transferred into both the DS and AS, and the co-culture system was fermented as a single strain (DSAS/CAB). Wild-type *E. coli* carrying pRB1s-CAB was used as control (Bw/CAB). The highest production rate of PHB obtained in the co-culture system was 0.54 g/(L·h), which is a two-fold increase over that in the wild-type strain (0.27 g/(L·h)). The PHB concentration in the co-culture system reached 26.04 g/L in 68 h, which was 3.06 times higher than that in wild-type strain (8.50 g/L) (Fig. 7C). The dry weight content of PHB (59.3%) and the conversion rate of glucose to PHB (17.61%) in the co-culture system were 2.70 times and 3.05 times higher than those of the wild-type strain (22.0% and 5.78%), respectively (Fig. 7D), which indicated that the TCA cycle was weakened and more Ac-CoA was redirected to synthesize PHB.

The relative oxygen consumption rate for the co-culture system (bioreactor 1) was compared with that for the wild-type control strain (bioreactor 2). The dissolved oxygen was automatically maintained at 30%, and therefore the relative oxygen consumption rate could be determined according to the agitating speed in each bioreactor. The results showed that the oxygen consumption rate of the co-culture system after induction was lower than that of the wild-type strain (Fig. 8A). Dissolved oxygen was kept at 30–50% by

auto-adjusted agitate (Fig. 8B). These findings showed that the co-culture system with a weakened TCA cycle directed more Ac-CoA to the PHB synthetic pathway and less carbon was being burned inefficiently through the TCA cycle, which showed that the co-culture system had better economical carbon efficiency than the wild-type strain.

3. Discussion

Co-culture systems have attracted increasing attention and have been widely used for modular metabolic engineering. In this study, we constructed three types of co-culture models. Notably, the unidirectional cross-feeding model, which is an often-overlooked model, was more conducive to the formation of a stable population ratio than the bidirectional cross-feeding. The key principles and factors that affected the ER were analyzed, and general principles for the establishment of a stable co-culture system were obtained. The principles can be applied to promote the progress of modular co-culture metabolic engineering research.

On the basis of the mathematical model theory, we developed a self-stable and population ratio adjustable co-culture system in this study, and showed that high cell density cultivation can be achieved, thereby overcoming the problems of instability and uncontrollable population ratio of traditional co-culture systems. The success of simulating multistage fermentation proves that the system can be scaled up to an industrial scale (see section 4 of Supplementary Information for details). The adjustable population ratio was vital for optimization of the inter-module, as was found for the synthesis of CGA. This also confirmed that the characteristics used to maintain a stable population ratio did not affect the expression of genes that encode exogenous proteins or pathway construction. To our knowledge, this is the first co-culture system for population ratio self-stability, adjustability, predictability, and scalability to be reported. The co-culture system provides a general platform for modularized co-culture engineering.

The ER of our co-culture system is, however, limited to within a certain range, and therefore, in future work, we will expand the adjustable range of the ER using genetic engineering strategies to adjust the correlation coefficient between bacteria and interactive substances. In particular, the ER was beyond the range in the co-culture systems with heterologous pathways (Fig. 5D), perhaps because of the metabolic burden that affected the secretion and absorption coefficients of AKG. Thus, rational use of metabolic burden is expected to be a promising strategy for regulating ER in the future studies.

Ac-CoA is located at the entrance of the TCA cycle in the metabolic pathway of *E. coli* and has been widely used for the biosynthesis of various value-added chemicals[41–43]. Completely blocking the TCA cycle to increase the abundance of Ac-CoA has been a commonly used strategy; however, the resultant poor growth affects the industrial production of Ac-CoA-derived chemicals. Weakening the TCA cycle by altering key gene promoters has also been used, but the disruption of the feedback regulation of gene expression led to metabolic disorders and hampered high cell density cultivation[41]. The DS-AS co-culture system developed in this study can be regarded as a symbiotic system, which not only reduced the flux of the TCA cycle but also retained the original regulatory elements. Such a design is difficult to achieve in a

single cell. The DS-AS co-culture system was successfully used to improve the PHB yield and conversion rate of glucose to PHB as well as reduce the oxygen consumption rate and emission of carbon dioxide. The low oxygen consumption and release of carbon dioxide make it a favorable system for industrial production in view of the increasing need for systems to be carbon neutral. This seems to be the first report of a manufactured symbiotic co-culture system being used to change the abundance of intracellular metabolites and achieve high production of target chemicals, and this provides a new insight into the application of co-culture systems. In addition to the accumulation of Ac-CoA, more cis-aconitic acid, citric acid, phenylpyruvate were obtained in the DS-AS co-culture system compared with the wild-type control strain, indicating the co-culture system can be applied for the enhanced production of other compounds.

Δ*sucA* and Δ*icd E. coli* strains have unique metabolic characteristics in single culture, and therefore they have many potential applications. For example, the Δ*icd* strain has more shunt in the glyoxylic acid cycle branch than wild-type *E. coli*, and is more conducive to the accumulation of glycolate[44] and glycine. The Δ*sucA* strain can accumulate more AKG than wild-type *E. coli*, and therefore could potentially be used to improve the yield of AKG-derived products[45,46]. However, these strains have a blocked TCA cycle, and therefore high cell density cultivation cannot be achieved when they are cultured separately using inexpensive cultivation methods, which limits their application. In this study, the high cell density cultivation of these two strains was realized simultaneously in the co-culture system, which provided a new approach for the culture of strains that are difficult to cultivate separately.

Other cross-feeding co-culture systems have been reported but they did not achieve good proportional stability[28,35]. Our mathematical model suggests that this may be because inappropriate interaction substances were used in their design. For example, acetate, as a bypass of central metabolism, is not suitable as an interactive substance because of the competitive inhibitory effect of glucose on acetate consumption. A variable acetate–biomass correlation coefficient under different glucose concentrations would lead to disorders of a co-culture system. A substance that is part of the central carbon metabolism pathway has more stable correlation coefficients and is more suitable as an interaction substance in co-culture systems, which is why we chose AKG as the interactive substance.

We found that unidirectional cross-feeding was more conducive to the formation of a stable population ratio than bidirectional cross-feeding, but this conclusion was based on a simple cross-feeding model. In nature, bidirectional cross-feeding is common and its population structure is generally stable mainly because symbionts often maintain the population ratio through complex feedback and regulation mechanisms. The main purpose of symbiotes in nature is survival in complex and changeable environments. Different from natural environments, the purpose of modular co-culture metabolic engineering is obtaining high yields of target products under artificially controlled conditions. An ideal co-culture system is one that is stable through simple genetic manipulation and one in which the population ratio can be controlled in a very simple way. However, the difficulty of adjusting population ratios artificially increases with the complexity of the symbiosis mechanism. Although a lot can be learned from natural symbiotic systems, because they have a different purpose, simply copying them may not be a

useful approach when designing modular co-culture metabolic engineering systems. Instead, a deeper consideration of what needs to be imitated and what should not be imitated from nature will contribute greatly to the development of efficient co-culture systems.

4. Methods

Strains

The strains and plasmids used in this study are listed in Table 1. *Escherichia coli K12* (BW25113) was used as the parental strain for genetic modification. The CRISPR-Cas9 system was used for DNA manipulation[47]. The exogenous genes were obtained by PCR amplification and ligased using the Gibson assembly method[48].

Table 1
Strains and plasmids used in this study

Strains	Description	Source
BW25113	rrnBT14ΔlacZWJ16hsdR514ΔaraBADAH33ΔrhaBADLD78	Invitrogen
Donor strain (DS)	BW25113, Δ*sucA*::P_{tac}-mCherry	This study
Acceptor strain (AS)	BW25113, Δ*icd*::P_{tac}-GFP	This study
CGA30	BW25113, Δ*ydiI*, harboring plasmid pCGA21	12
CGADS	DS, Δ*ydiI*, harboring plasmid pCGA21	This study
CGAAS	AS, Δ*ydiI*, harboring plasmid pCGA21	This study
Bw/CAB	BW25113 harboring pRB1s-CAB	This study
DS/CAB	DS harboring pRB1s-CAB	This study
AS/CAB	AS harboring pRB1s-CAB	This study
CADS	DS, ΔtyrR, harboring pCA	This study
CAAS	AS, ΔtyrR, harboring pCA	This study
Plasmids	**Description**	**Source**
pRB1s	araBAD promoter, RSF1030 ori, Str^r	our lab
pYB1k	araBAD promoter, p15A ori, Kan^r	our lab
pRB1s-CAB	pRB1s containing PhaC from *Pseudomonas stutzeri*, PhaA and PhaB from *Ralstonia eutropha*	This study, 49,50
pCA	pYB1k containing HpaBC from *E. coli* MG1655 and TAL from *Saccharothrix espanaensis*	This study, 12
pCGA21	HQT expressed from promoter P_{119}, 4CL2 expressed from promoter P_{GAP}, ColA ori	12

DS, donor strain; AS, acceptor strain; Bw, *E. coli* BW25113; pCGA21, plasmid carrying chlorogenic acid synthesis module; pCA, plasmid carrying caffeic acid synthesis module; pRB1s-CAB, poly-β-hydroxybutyrate (PHB) synthesizes related plasmids carrying *phaA*, *phaB*, and *phaC* genes.

Chemicals

T4 DNA ligase, Gibson kits, and restriction enzymes were purchased from New England Biolabs (USA). Plasmid extraction and gel purification kits were purchased from Omega (Beijing, China). DNA polymerase (2× High Fidelity Master Mix) was purchased from TSINGKE (Beijing, China). Media

components were purchased from Becton–Dickinson (Beijing, China). Standards of Glucose, PHB, CGA, CA and other chemicals were obtained from Sigma-Aldrich (Shanghai, China).

Media

Luria–Bertani (LB) medium

Tryptone 10 g/L, NaCl 10 g/L, and yeast extract 5 g/L.

Modified inorganic salts medium (chemically defined (CD) medium) for small scale culture

Glucose 10 g/L, KH_2PO_4 14 g/L, $(NH_4)_2PO_4$ 4 g/L, $MgSO_4 \cdot 7H_2O$ 0.6 g/L, and trace elements [8.4 mg/L EDTA, 2.5 mg/L $CoCl_2 \cdot 6H_2O$, 15 mg/L $MnCl_2 \cdot 4H_2O$, 1.5 mg/L $CuCl_2 \cdot 2H_2O$, 3 mg/L H_3BO_3, 2.5 mg/L $Na_2MoO_4 \cdot 2H_2O$, 13 mg/L $Zn(CH_3COO)_2 \cdot 2H_2O$, and 100 mg/L Fe^{3+} + citrate]. To adjust the pH to 7.4 before the cultures were autoclaved, 5 M $NH_3 \cdot H_2O$ was used.

CD medium for fermentation

Glucose 20 g/L, KH_2PO_4 14 g/L, $(NH_4)_2PO_4$ 4 g/L, $MgSO_4 \cdot 7H_2O$ 0.6 g/L, and trace elements [8.4 mg/L EDTA, 2.5 mg/L $CoCl_2 \cdot 6H_2O$, 15 mg/L $MnCl_2 \cdot 4H_2O$, 1.5 mg/L $CuCl_2 \cdot 2H_2O$, 3 mg/L H_3BO_3, 2.5 mg/L $Na_2MoO_4 \cdot 2H_2O$, 13 mg/L $Zn(CH_3COO)_2 \cdot 2H_2O$, and 100 mg/L Fe^{3+} + citrate]. To adjust the pH to 7.0, 5 M $NH_3 \cdot H_2O$ was used. For the fed-batch fermentation, the feeding medium contained 600 g/L glucose, 2 g/L $MgSO_4 \cdot 7H_2O$, and trace elements [13 mg/L EDTA, 4 mg/L $CoCl_2 \cdot 6H_2O$, 23.5 mg/L $MnCl_2 \cdot 4H_2O$, 2.5 mg/L $CuCl_2 \cdot 2H_2O$, 5 mg/L H_3BO_3, 4 mg/L $Na_2MoO_4 \cdot 2H_2O$, 16 mg/L $Zn(CH_3COO)_2 \cdot 2H_2O$, and 40 mg/L Fe^{3+} + citrate].

LB solid medium and CD solid medium

These media were the same as the corresponding liquid medium with 2% AGAR powder added.

All the above media were supplemented with antibiotics corresponding to the strains, with doses of Streptomycin sulfate (Str) 50 mg/L and Kanamycin sulfate (Kan) 50 mg/L.

Culture conditions

Molecular construction and strain cultivation

Strains were grown in LB medium at 37°C and 220 rpm unless otherwise stated.

Symbiotic phenomenon display test in solid medium

Strains were pre-cultured in LB medium for 6–8 h. Cells were harvested by centrifugation at 4000 × g for 10 min and resuspended in an equal volume of 0.85% NaCl solution. Then, 20 μL of the first strain suspension was dropped into one side of the CD solid medium, and the plate was turned gently so that the liquid diffused into a uniform circle. After the first solution dried, 20 μL of the second strain

suspension was dropped into the other side of the medium. The plate was turned gently and left to dry. The margins of the two bacterial suspensions should be as close as possible, but not in contact. The inoculated solid plates were incubated at 37°C overnight. Images of each agar plate were captured using an inhouse multi-color fluorescent imager.

Shake flask test in CD medium

Strains were pre-cultured in LB medium for 6–8 h. Cells were harvested by centrifugation at 4000 × g for 10 min, resuspended in an equal volume of 0.85% NaCl solution, and then transferred into 50 mL CD medium with 1% total inoculum in a 500-ml shake flask with baffle and incubated at 37℃ and 220 rpm for more than 12 h.

Fed-batch fermentation in bioreactor

Strains were initially cultured in LB medium at 37°C and 220 rpm to a biomass of OD_{600} = 1.5–2 to produce a seed culture. Then, the seed culture was inoculated into 500 mL CD medium in a 1-L fermenter (Bailun Biotechnology Co., Ltd, Shanghai, China) with a total inoculation ratio of 4%. Each strain was cultivated independently, and the ratio of each strain in the co-culture was 1:1 unless otherwise noted. The fermentation was conducted at 37°C with the pH controlled at 7.0 by the automatic addition of 5 M NH3·H2O. The dissolved oxygen level was maintained at 30% (v/v) by air flow at 0.5–1 L/min and by changing the agitation speed from 500 to 1200 rpm automatically. When the initial glucose was exhausted and the dissolved oxygen value rose sharply, feeding started at a constant rate of 5 g/(L·h) of glucose. Fermentation was considered complete when the biomass no longer increased.

PHB and CGA production in the bioreactor

Seed preparation and initial fermentation conditions were the same as those described above. The feeding rate was set at 4 g/(L·h) of glucose as an initial value, and then increased by 1.2 times every 2 h. When the dissolved oxygen did not fluctuate positively with the feeding, the feeding rate was reduced to ensure that no glucose accumulated. The maximum feeding rate did not exceed 10 g/(L·h). When the biomass at OD_{600} = 30, the fermentation temperature was lowered to 30°C, and L-arabinose (2 g/L) was added into the culture as inducer. For PHB production, the identical feeding and induction scheme was used for the co-culture system and the wild-type control strain. For CGA production, 2 g/L of quinic acid was added during induction.

Model development

The mathematic model of the co-culture system was established using the Python programming language and the SymPy, NumPy, Pandas, and Matplotlib packages. Cell growth, substance consumption, and release all followed the modified Monod model[51,52]. An iterative method was used to simulate the culture process at a time interval of 0.01 h. Derivation and analysis of the mathematical model are provided as supplementary information.

Analytical methods

Cell density

Cell density was estimated by measuring optical density at 600 nm with a spectrophotometer.

Quantification of extracellular metabolites

Concentrations of glucose in culture supernatant were measured by high-performance liquid chromatography (HPLC) with a Bio-Rad Aminex HPX-87 H column (7.8×300 mm; Hercules, CA, USA) with a refractive index detector and a diode array detector (210 nm). The analysis was performed with a flow rate of 0.6 mL/min using 5 mM H_2SO_4 as the mobile phase at 55°C.

Quantification of intracellular metabolites

Samples were collected when the bacteria were in the stable state of high-density fermentation. The bacteria (90 OD) were centrifuged and washed twice with normal saline, then suspended in 1 mL methanol (90%), followed by ultrasonic crushing and vacuum drying. Metabolites were detected by liquid-phase mass spectrometry.

Quantification of dry cell weight and PHB

After culturing, the cells were harvested and the dry cell weight was measured. The PHB samples were treated following the method used in a previous study[53]. The HPLC method described above was used to quantify the extracellular metabolites. The amount of crotonic acid produced from PHB was calculated from the regression equation derived from the known standard PHB obtained from Sigma-Aldrich.

Quantification of CA and CGA

CGA and CA productions were analyzed by HPLC. The culture broth was centrifuged for 10 min at 10,000 × g, and the supernatant was filtered through a 0.22-μm filter prior to HPLC analysis. A Shimadzu LC-20A HPLC system (Shimadzu Corp., Kyoto, Japan) equipped with an SPD-M20A photodiode array detector operating at 327 nm was used to quantify CGA and CA. Separation of products was achieved with a Waters Symmetry C18 column (250×4.6 mm, 5 μm) working at 35°C, with a mobile phase of 25% methanol in 0.05% (vol/vol) acetic acid at a flow rate of 0.4 mL/min. The CGA and CA concentrations were calculated using standard curves prepared with authentic CGA and CA.

Quantification of DS and AS cell numbers

The population ratio in the co-culture system was detected by flow cytometry. Cells samples were collected and washed twice using PBS buffer (per liter: 0.24 g KH2PO4, 1.44 g Na2HPO4, 8 g NaCl, 0.2 g KCl, pH 7.4) and diluted with PBS buffer to a cell concentration of OD_{600nm} = 0.2–0.5. Flow cytometry influx was used to detect the proportion of strains with different fluorescent proteins. Strains labeled with

GFP were detected using the FITC channel (530_40-[488_200]), and strains labeled with mCherry were detected using the PE channel (593_40-[561_150]).

Statistical analysis

Values are shown as mean ± standard deviation from three (n = 3) biological replicates (Fig. 3C, D) and two (n = 2) biological replicates (Figs. 4B, D–F, 5B, C, 6A–D, 7A, C, D). Two-tailed t tests were used to determine statistical significance, which was indicated for $P < 0.05$.

5. Data Availability

Data supporting the findings of this study are available within the article and Supplementary Information or from the corresponding author upon reasonable request. Source data are provided with this paper.

Declarations

Acknowledgments

We thank Huiwei Zhao for providing the multi-color fluorescent imager. We thank Margaret Biswas, PhD, from Liwen Bianji (Edanz) (www.liwenbianji.cn/) for editing the English text of a draft of this manuscript.

Author contributions

H.C. conceived and designed the project, developed the model, designed the experiments, carried out bacteria culture and product detection, and drafted the manuscript; Q.L. constructed the plasmids and strains related to PHB synthesis and revised the manuscript; S.T. and S.L. constructed the plasmids and strains related to CGA synthesis; X.W. assisted in the fermentation experiments; Y.T. supervised the whole project; B.L. and W.L. co-supervised the experiments and revised the manuscript.

References

1 Ramzi, A. B. Metabolic Engineering and Synthetic Biology. *Advances in experimental medicine and biology* **1102**, 81-95, doi:10.1007/978-3-319-98758-3_6 (2018).

2 Woolston, B. M., Edgar, S. & Stephanopoulos, G. Metabolic engineering: past and future. *Annual review of chemical and biomolecular engineering* **4**, 259-288, doi:10.1146/annurev-chembioeng-061312-103312 (2013).

3 Goers, L., Freemont, P. & Polizzi, K. M. Co-culture systems and technologies: taking synthetic biology to the next level. *J R Soc Interface* **11**, doi:10.1098/rsif.2014.0065 (2014).

4 Zhang, H. & Wang, X. Modular co-culture engineering, a new approach for metabolic engineering. *Metab Eng* **37**, 114-121, doi:10.1016/j.ymben.2016.05.007 (2016).

5 Jones, J. A. & Wang, X. Use of bacterial co-cultures for the efficient production of chemicals. *Current opinion in biotechnology* **53**, 33-38, doi:10.1016/j.copbio.2017.11.012 (2018).

6 McCarty, N. S. & Ledesma-Amaro, R. Synthetic Biology Tools to Engineer Microbial Communities for Biotechnology. *Trends Biotechnol* **37**, 181-197, doi:10.1016/j.tibtech.2018.11.002 (2019).

7 Qian, X. *et al.* Biotechnological potential and applications of microbial consortia. *Biotechnology advances* **40**, 107500, doi:10.1016/j.biotechadv.2019.107500 (2020).

8 Wu, G. *et al.* Metabolic Burden: Cornerstones in Synthetic Biology and Metabolic Engineering Applications. *Trends Biotechnol* **34**, 652-664, doi:10.1016/j.tibtech.2016.02.010 (2016).

9 Artsatbanov, V. Y. *et al.* Influence of oxidative and nitrosative stress on accumulation of diphosphate intermediates of the non-mevalonate pathway of isoprenoid biosynthesis in corynebacteria and mycobacteria. *Biochemistry. Biokhimiia* **77**, 362-371, doi:10.1134/s0006297912040074 (2012).

10 Tsoi, R. *et al.* Metabolic division of labor in microbial systems. *Proc Natl Acad Sci U S A* **115**, 2526-2531, doi:10.1073/pnas.1716888115 (2018).

11 Camacho-Zaragoza, J. M. *et al.* Engineering of a microbial coculture of Escherichia coli strains for the biosynthesis of resveratrol. *Microb Cell Fact* **15**, 163, doi:10.1186/s12934-016-0562-z (2016).

12 Li, S. *et al.* De Novo Biosynthesis of Chlorogenic Acid Using an Artificial Microbial Community. *J Agric Food Chem* **69**, 2816-2825, doi:10.1021/acs.jafc.0c07588 (2021).

13 Zhang, Y. *et al.* Notable Improvement of 3-Hydroxypropionic Acid and 1,3-Propanediol Coproduction Using Modular Coculture Engineering and Pathway Rebalancing. *ACS Sustainable Chemistry & Engineering* **9**, 4625-4637, doi:10.1021/acssuschemeng.1c00229 (2021).

14 Liu, Y. *et al.* A three-species microbial consortium for power generation. *Energy & Environmental Science* **10**, 1600-1609, doi:10.1039/c6ee03705d (2017).

15 Ganesan, V., Li, Z., Wang, X. & Zhang, H. Heterologous biosynthesis of natural product naringenin by co-culture engineering. *Synth Syst Biotechnol* **2**, 236-242, doi:10.1016/j.synbio.2017.08.003 (2017).

16 Jones, J. A. *et al.* Experimental and computational optimization of an Escherichia coli co-culture for the efficient production of flavonoids. *Metabolic Engineering* **35**, 55-63, doi:https://doi.org/10.1016/j.ymben.2016.01.006 (2016).

17 Shin, H. D., McClendon, S., Vo, T. & Chen, R. R. Escherichia coli binary culture engineered for direct fermentation of hemicellulose to a biofuel. *Appl Environ Microbiol* **76**, 8150-8159,

doi:10.1128/AEM.00908-10 (2010).

18 Minty, J. J. *et al.* Design and characterization of synthetic fungal-bacterial consortia for direct production of isobutanol from cellulosic biomass. *Proc Natl Acad Sci U S A* **110**, 14592-14597, doi:10.1073/pnas.1218447110 (2013).

19 Bayer, T. S. *et al.* Synthesis of methyl halides from biomass using engineered microbes. *Journal of the American Chemical Society* **131**, 6508-6515, doi:10.1021/ja809461u (2009).

20 Liu, X. *et al.* Convergent engineering of syntrophic Escherichia coli coculture for efficient production of glycosides. *Metab Eng* **47**, 243-253, doi:10.1016/j.ymben.2018.03.016 (2018).

21 Zhang, H., Pereira, B., Li, Z. & Stephanopoulos, G. Engineering Escherichia coli coculture systems for the production of biochemical products. *Proc Natl Acad Sci U S A* **112**, 8266-8271, doi:10.1073/pnas.1506781112 (2015).

22 Scott, S. R. *et al.* A stabilized microbial ecosystem of self-limiting bacteria using synthetic quorum-regulated lysis. *Nature microbiology* **2**, 17083, doi:10.1038/nmicrobiol.2017.83 (2017).

23 Scott, S. R. & Hasty, J. Quorum Sensing Communication Modules for Microbial Consortia. *ACS Synth Biol* **5**, 969-977, doi:10.1021/acssynbio.5b00286 (2016).

24 Balagadde, F. K. *et al.* A synthetic Escherichia coli predator-prey ecosystem. *Mol Syst Biol* **4**, 187, doi:10.1038/msb.2008.24 (2008).

25 Abisado, R. G., Benomar, S., Klaus, J. R., Dandekar, A. A. & Chandler, J. R. Bacterial Quorum Sensing and Microbial Community Interactions. *mBio* **9**, doi:10.1128/mBio.02331-17 (2018).

26 Ng, W. L. & Bassler, B. L. Bacterial quorum-sensing network architectures. *Annu Rev Genet* **43**, 197-222, doi:10.1146/annurev-genet-102108-134304 (2009).

27 Zhang, W. *et al.* Production of naringenin from D-xylose with co-culture of E. coli and S. cerevisiae. *Eng Life Sci* **17**, 1021-1029, doi:10.1002/elsc.201700039 (2017).

28 Zhou, K., Qiao, K., Edgar, S. & Stephanopoulos, G. Distributing a metabolic pathway among a microbial consortium enhances production of natural products. *Nat Biotechnol* **33**, 377-383, doi:10.1038/nbt.3095 (2015).

29 Pande, S. *et al.* Fitness and stability of obligate cross-feeding interactions that emerge upon gene loss in bacteria. *ISME J* **8**, 953-962, doi:10.1038/ismej.2013.211 (2014).

30 Mee, M. T., Collins, J. J., Church, G. M. & Wang, H. H. Syntrophic exchange in synthetic microbial communities. *Proc Natl Acad Sci U S A* **111**, E2149-2156, doi:10.1073/pnas.1405641111 (2014).

31 Kerner, A., Park, J., Williams, A. & Lin, X. N. A programmable Escherichia coli consortium via tunable symbiosis. *PLoS One* **7**, e34032, doi:10.1371/journal.pone.0034032 (2012).

32 Bernstein, H. C., Paulson, S. D. & Carlson, R. P. Synthetic Escherichia coli consortia engineered for syntrophy demonstrate enhanced biomass productivity. *J Biotechnol* **157**, 159-166, doi:10.1016/j.jbiotec.2011.10.001 (2012).

33 Wintermute, E. H. & Silver, P. A. Emergent cooperation in microbial metabolism. *Mol Syst Biol* **6**, 407, doi:10.1038/msb.2010.66 (2010).

34 Shou, W., Ram, S. & Vilar, J. M. Synthetic cooperation in engineered yeast populations. *Proc Natl Acad Sci U S A* **104**, 1877-1882, doi:10.1073/pnas.0610575104 (2007).

35 Losoi, P. S., Santala, V. P. & Santala, S. M. Enhanced Population Control in a Synthetic Bacterial Consortium by Interconnected Carbon Cross-Feeding. *ACS Synth Biol* **8**, 2642-2650, doi:10.1021/acssynbio.9b00316 (2019).

36 Brenner, K., You, L. & Arnold, F. H. Engineering microbial consortia: a new frontier in synthetic biology. *Trends Biotechnol* **26**, 483-489, doi:10.1016/j.tibtech.2008.05.004 (2008).

37 Hanemaaijer, M. *et al.* Systems modeling approaches for microbial community studies: from metagenomics to inference of the community structure. *Frontiers in Microbiology* **6**, doi:10.3389/fmicb.2015.00213 (2015).

38 Noor, E., Eden, E., Milo, R. & Alon, U. Central carbon metabolism as a minimal biochemical walk between precursors for biomass and energy. *Mol Cell* **39**, 809-820, doi:10.1016/j.molcel.2010.08.031 (2010).

39 Creaghan, I. T. & Guest, J. R. Succinate dehydrogenase-dependent nutritional requirement for succinate in mutants of Escherichia coli K12. *J Gen Microbiol* **107**, 1-13, doi:10.1099/00221287-107-1-1 (1978).

40 Venditti, V., Ghirlando, R. & Clore, G. M. Structural basis for enzyme I inhibition by alpha-ketoglutarate. *ACS Chem Biol* **8**, 1232-1240, doi:10.1021/cb400027q (2013).

41 Krivoruchko, A., Zhang, Y., Siewers, V., Chen, Y. & Nielsen, J. Microbial acetyl-CoA metabolism and metabolic engineering. *Metab Eng* **28**, 28-42, doi:10.1016/j.ymben.2014.11.009 (2015).

42 Zhang, S. *et al.* Metabolic engineering for efficient supply of acetyl-CoA from different carbon sources in Escherichia coli. *Microb Cell Fact* **18**, 130, doi:10.1186/s12934-019-1177-y (2019).

43 Martin, V. J., Pitera, D. J., Withers, S. T., Newman, J. D. & Keasling, J. D. Engineering a mevalonate pathway in Escherichia coli for production of terpenoids. *Nat Biotechnol* **21**, 796-802, doi:10.1038/nbt833 (2003).

44 Zhu, T. *et al.* Multiple strategies for metabolic engineering of Escherichia coli for efficient production of glycolate. *Biotechnol Bioeng* **118**, 4699-4707, doi:10.1002/bit.27934 (2021).

45 Luo, H. *et al.* Microbial production of gamma-aminobutyric acid: applications, state-of-the-art achievements, and future perspectives. *Crit Rev Biotechnol* **41**, 491-512, doi:10.1080/07388551.2020.1869688 (2021).

46 Sirisansaneeyakul, S. *et al.* Microbial production of poly-gamma-glutamic acid. *World J Microbiol Biotechnol* **33**, 173, doi:10.1007/s11274-017-2338-y (2017).

47 Jiang, Y. *et al.* Multigene editing in the Escherichia coli genome via the CRISPR-Cas9 system. *Appl Environ Microbiol* **81**, 2506-2514, doi:10.1128/AEM.04023-14 (2015).

48 Gibson, D. G. *et al.* Enzymatic assembly of DNA molecules up to several hundred kilobases. *Nat Methods* **6**, 343-345, doi:10.1038/nmeth.1318 (2009).

49 Liu, Q., Ouyang, S. P., Chung, A., Wu, Q. & Chen, G. Q. Microbial production of R-3-hydroxybutyric acid by recombinant E. coli harboring genes of phbA, phbB, and tesB. *Appl Microbiol Biotechnol* **76**, 811-818, doi:10.1007/s00253-007-1063-0 (2007).

50 Gao, X. *et al.* Production of copolyesters of 3-hydroxybutyrate and medium-chain-length 3-hydroxyalkanoates by E. coli containing an optimized PHA synthase gene. *Microb Cell Fact* **11**, 130, doi:10.1186/1475-2859-11-130 (2012).

51 Monod, J. THE GROWTH OF BACTERIAL CULTURES. *Annual Review of Microbiology* **3**, 371-394, doi:10.1146/annurev.mi.03.100149.002103 (1949).

52 Liu, Y. Overview of some theoretical approaches for derivation of the Monod equation. *Appl Microbiol Biotechnol* **73**, 1241-1250, doi:10.1007/s00253-006-0717-7 (2007).

53 Masood, F., Yasin, T. & Hameed, A. Production and Characterization of Tailor-Made Polyhydroxyalkanoates by Bacillus cereus FC11. *pakistan journal of zoology* **47**, 491-503 (2015).

Figures

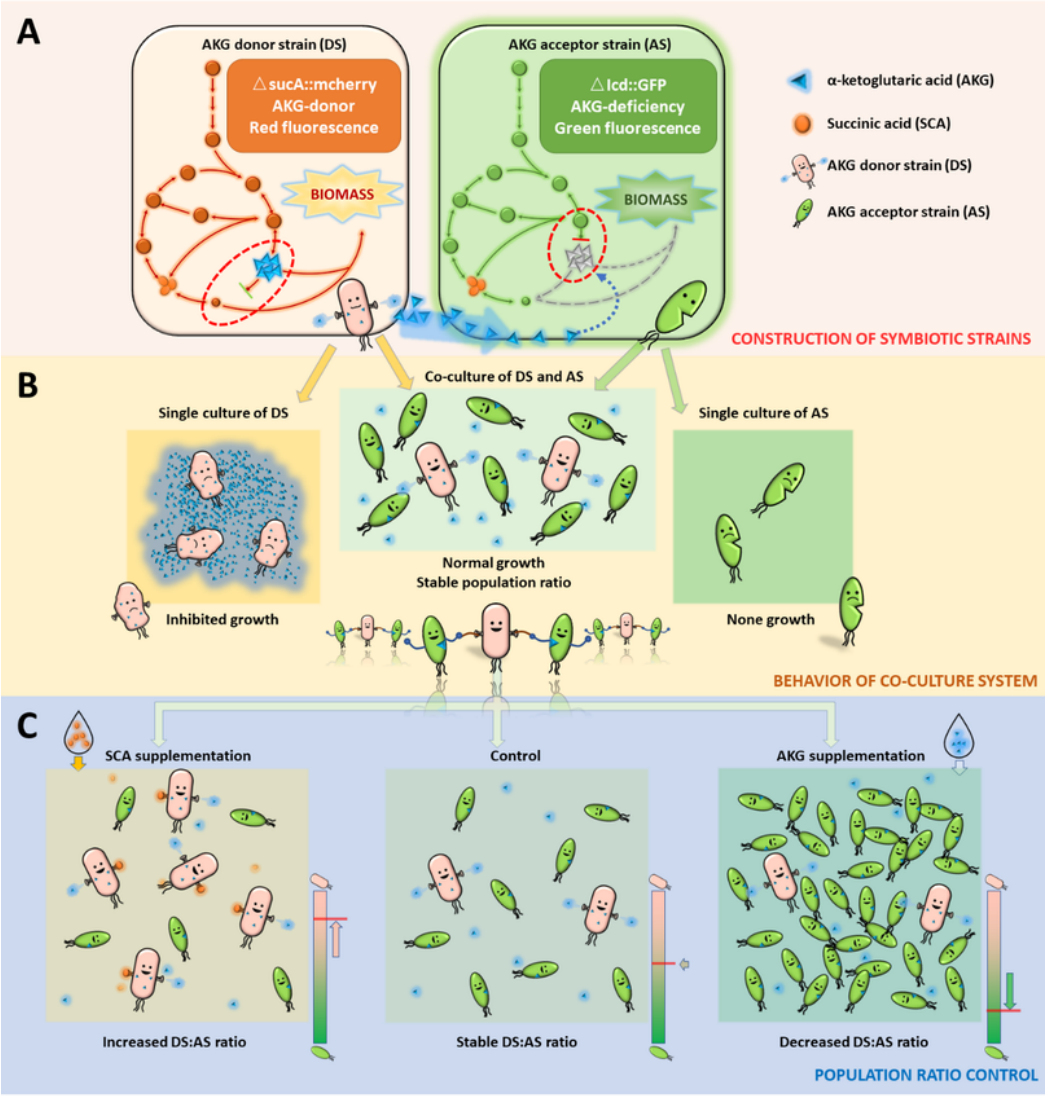

Figure 1

Schematic overview of DS-AS co-culture system. (A) Construction of symbiotic E. coli strains. The α-ketoglutaric acid (AKG) donor strain (DS) is a *sucA*-knockout strain with constitutively expressed red fluorescent protein (mCherry). The DS cannot express 2-ketoglutarate dehydrogenase and tends to accumulate AKG. The AKG acceptor strain (AS) is an *icd*-knockout strain with constitutively expressed green fluorescent protein (GFP). The growth of AS depends on the uptake of AKG from the environment.

(B) Behavior of the DS-AS co-culture system. The DS and AS do not grow well in single culture; whereas, in the DS-AS co-culture, normal growth is achieved and the population ratio remains stable. (C) Population ratio control. The population ratio (DS:AS) was up-regulated by adding succinic acid (SCA) and down-regulated by adding AKG into the culture system.

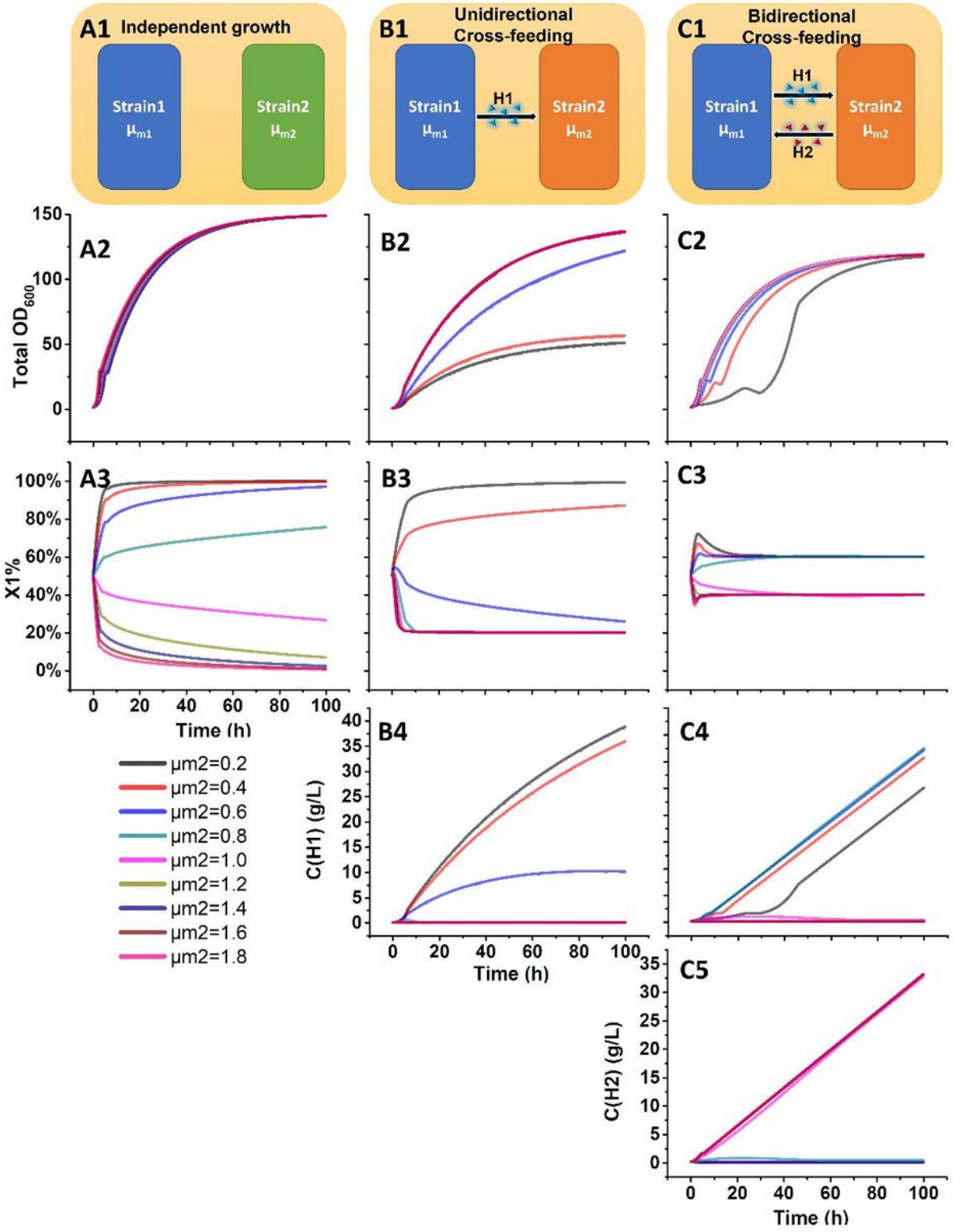

Figure 2

Schematic overview and trend prediction on different maximum specific growth rate of Strain2 (μ_{m2}) of three co-culture models. (A1–C1) Schematic overview of independent growth, unidirectional cross-feeding, bidirectional cross-feeding. (A2–C2) Total OD_{600} biomass by prediction. (A3–C3) Population ratio of Strain1 by prediction. (B4, C4) Concentration of interactive substance H1 by prediction. (C5) Concentration of interactive substance H2 by prediction. (Details of the mathematical models are provided as Supplementary Information.)

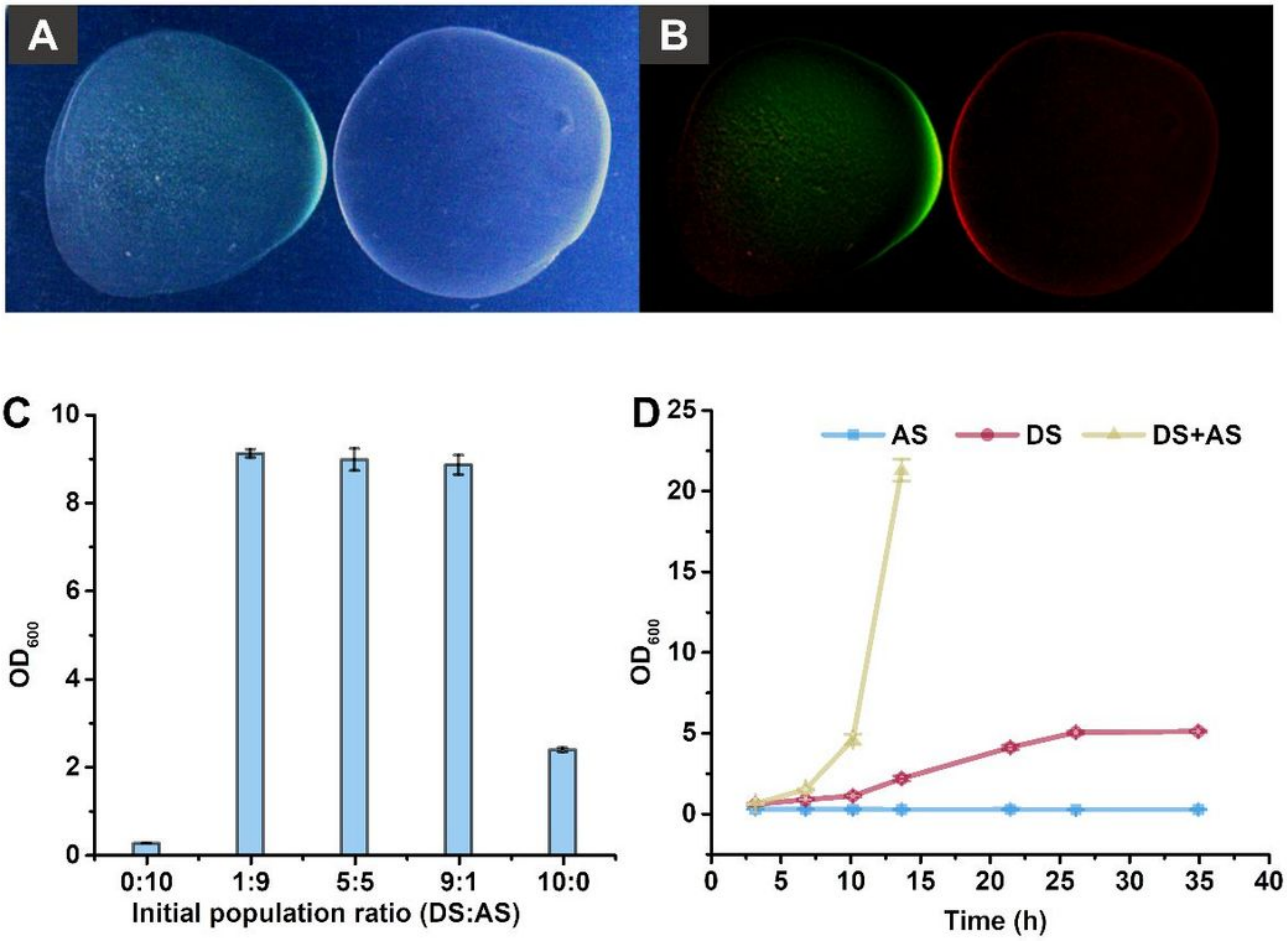

Figure 3

Identification of symbiotic relationship in the DS-AS co-culture system. (A, B) Non-contact spreading tests on solid medium. The acceptor strain (AS, green) is on the left, and the donor strain (DS, red) is on the right. Visible light photograph (A) and fluorescence images (B) taken separately and later overlayed by Python programming language. (C) Identification of system symbiotic relationship at shaker scale. (D) Identification of system symbiotic relationship at batch bioreactor scale. Error bars indicate the standard deviation of triplicate cultures.

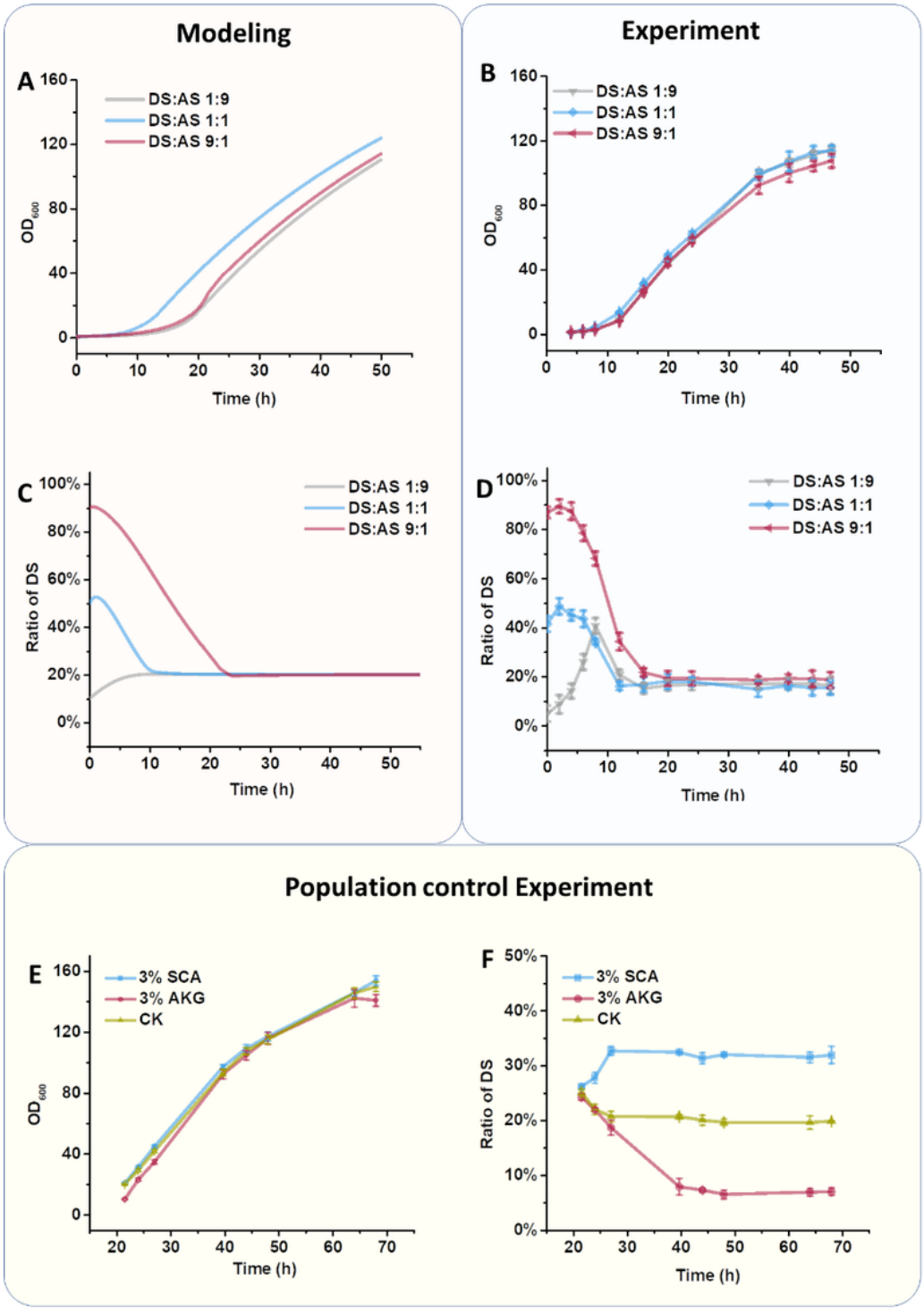

Figure 4

Model prediction and experimental data of the DS-AS co-culture system at the fed-batch bioreactor scale. (A) Predicted total OD600 of the DS and AS in the co-culture system. (B) Experimental total OD600 of the DS and AS in the co-culture system. (C) Proportion of the DS in the co-culture system predicted by the model. (D) Experimentally determined proportion of the DS in the co-culture system. (E, F) Adjustment of equilibrium population ratio by supplementing the feeding medium with α-ketoglutaric acid (AKG) or

succinic acid (SCA). 3% SCA, 3% SCA added in feeding medium (containing 60% glucose); 3% AKG, 3% AKG added in feeding medium; CK, without population ratio control (no additional substance in the feeding medium). Error bars indicated the standard deviation of duplicate cultures.

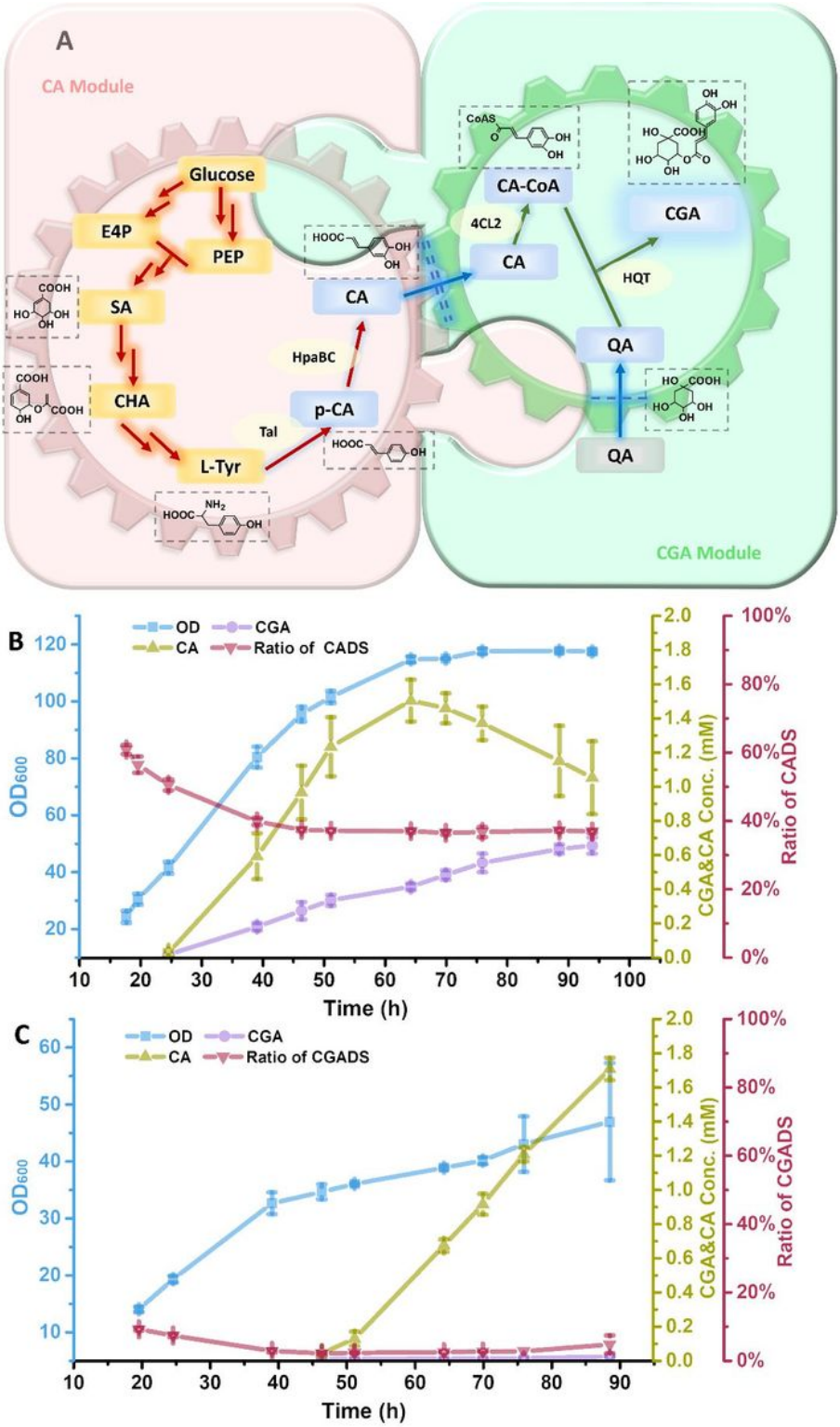

Figure 5

Schematic diagram of the chlorogenic acid (CGA) biosynthesis pathway in *E. coli* and CGA production in a 1-L fed-batch bioreactor. (A) The CGA biosynthesis pathway in *E. coli*. Heterologous genes introduced to reconstitute the pathway are indicated in yellow. TAL, tyrosine ammonia lyase; HpaBC, 4-hydroxyphenylacetate 3-hydroxylase; 4CL, p-coumarate:CoA ligase; HQT, hydroxycinnamoyl-CoA quinate transferase; PEP, phosphoenolpyruvate; E4P, D-erythrose-4-phosphate; SA, shikimic acid; CHA, chorismite acid; L-Tyr, L-tyrosine; QA, quinic acid; p-CA, p-coumaric acid; CA, caffeic acid; CA-CoA, caffeoyl-CoA; CGA, chlorogenic acid. (B, C) CGA production in a -L fed-batch bioreactor without population control. (B) Combination 1, co-culture of CADS and CGAAS without inter-module adjustment. CADS, DS Δ*tyrR*, harboring plasmid pCA (pYB1k containing HpaBC from *E. coli* MG1655 and TAL from *Saccharothrix espanaensis*); CGAAS, AS Δ*ydiI*, harboring plasmid pCGA21 (a plasmid with HQT expressed from promoter P1194CL2 expressed from promoter PGAP, ColA ori). (C) Combination 2, co-culture of CAAS (AS Δ*tyrR*, harboring plasmid pCA) and CGADS (DS Δ*ydiI,* harboring plasmid pCGA21) without inter-module adjustment. Error bars indicate the standard deviation of duplicate cultures.

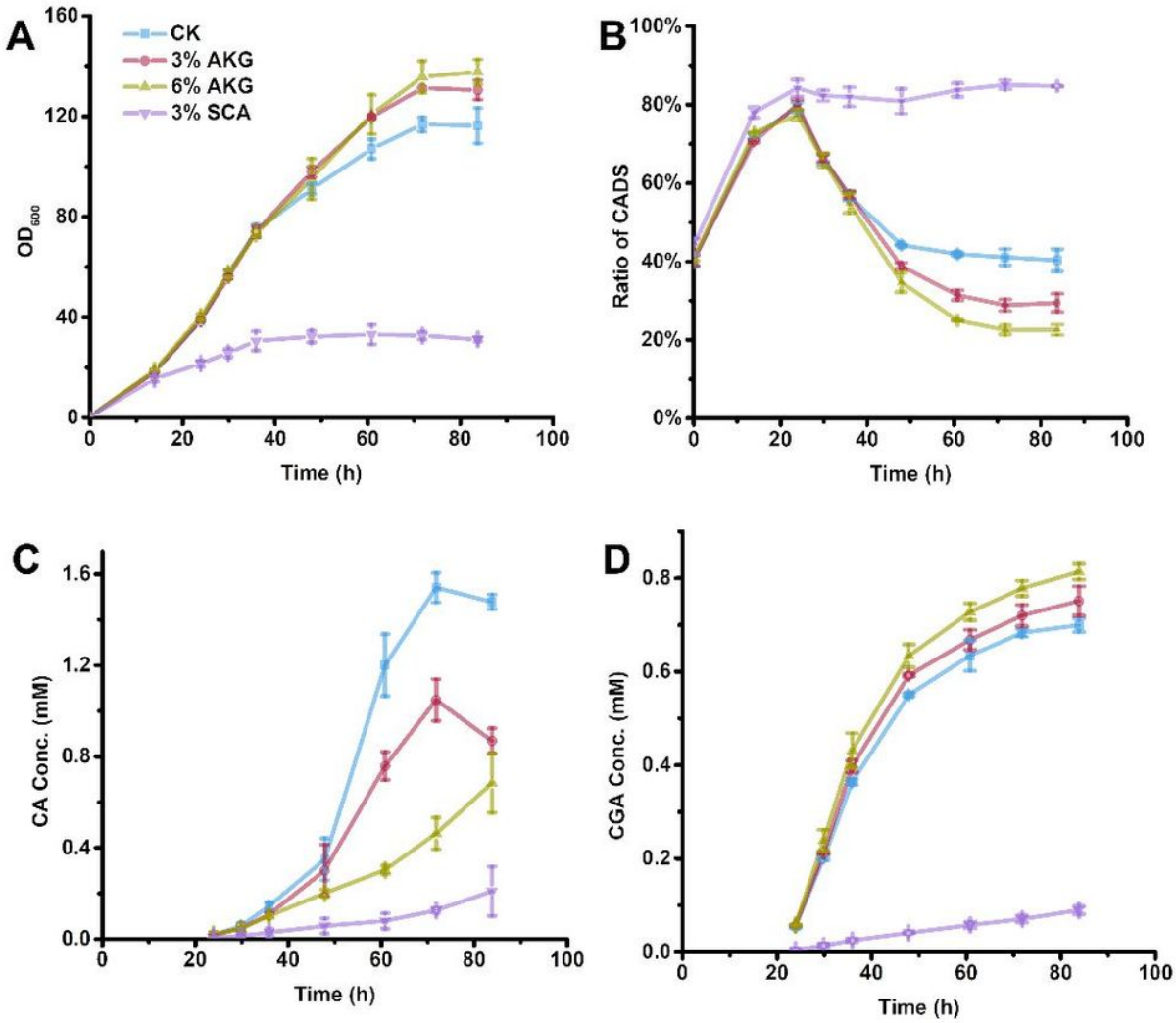

Figure 6

Chlorogenic acid (CGA) production with population ratio control by combination 1. Changes in (A) OD_{600}, (B) ratio of CADS (DS Δ*tyrR*, harboring plasmid pCA), (C, D) concentrations of caffeic acid (CA) and CGA over time. 3% AKG, 3% α-ketoglutaric acid added in feeding medium; 6% AKG, 6% AKG added in feeding medium; 3% SCA, 3% succinic acid added in feeding medium; CK, without population ratio control. Error bars indicate the standard deviation of duplicate cultures.

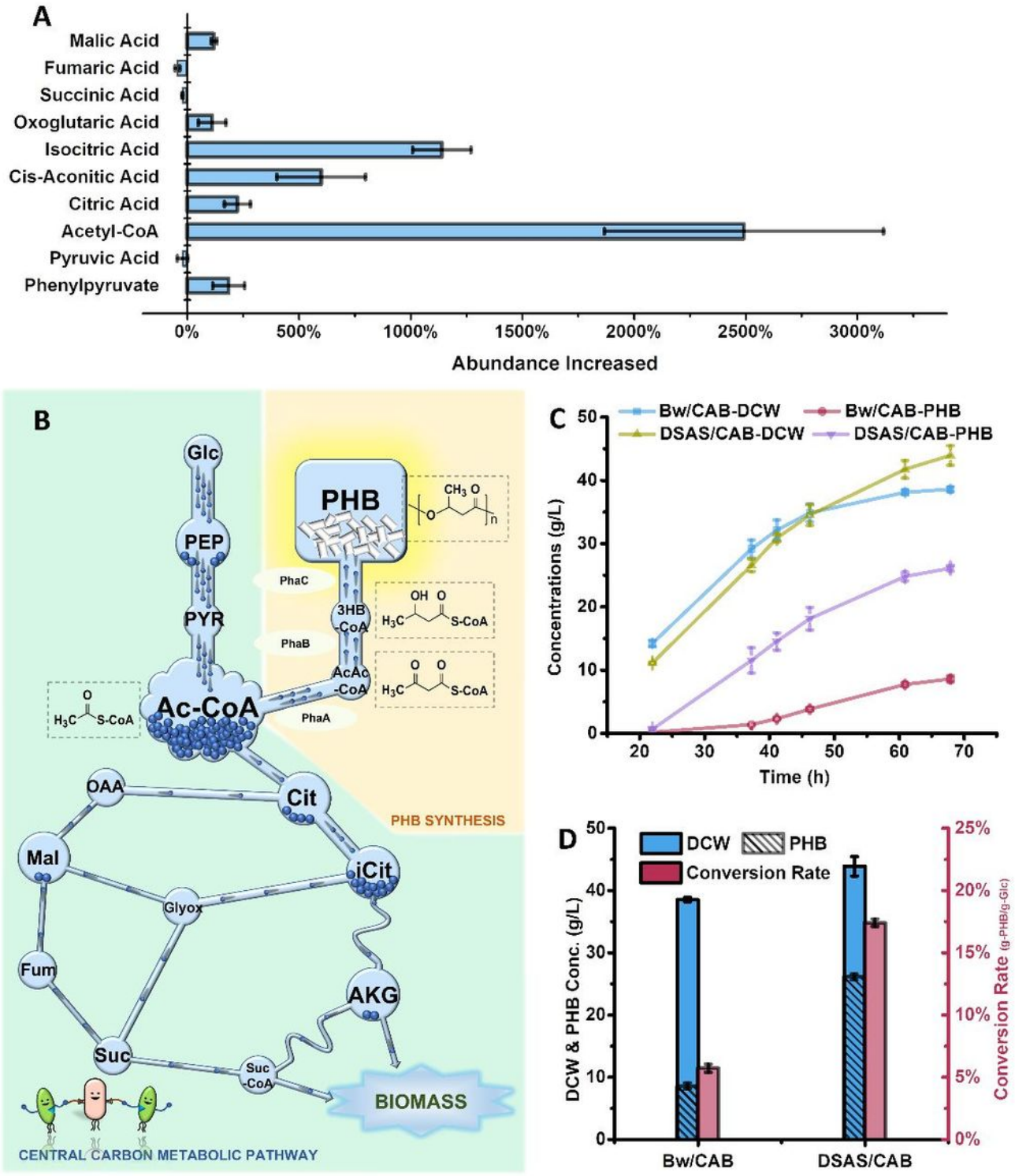

Figure 7

Enhanced poly-β-hydroxybutyrate (PHB) production benefited by the metabolic characteristics of the co-culture system. (A) Increased ratios of intracellular metabolite abundance in the DS-AS co-culture system compared with those in the wild-type strain measured by metabolomics. (B) Schematic diagram of metabolism and the PHB synthesis pathway in the DS-AS co-culture system. PhaA, acetyl-CoA C-acetyltransferase; PhaB, acetoacetyl-CoA reductase; PhaC, poly[(R)-3-hydroxyalkanoate] polymerase subunit; PEP, phosphoenolpyruvate; PYR, pyruvate; Ac-CoA, acetyl-CoA; Cit, citric acid; iCit, isocitric acid; AKG, α -ketoglutaric acid; SucCoA, succinyl-coA; Suc, succinic acid; Fum, fumaric acid; Mal, malic acid, OAA, oxaloacetic acid; Glyox, glyoxylic acid; AcAc-CoA, acetoacetyl-CoA; (R)-3HB-CoA, (R)-3-hydroxybutyrate CoA; PHB, poly-β-hydroxybutyric acid. (C) Cell dry weight (DCW) and PHB production in a 1-L fed-batch bioreactor. Bw/CAB, BW25113 harboring pRB1s-CAB (pRB1s containing PhaC from *Pseudomonas stutzeri*, and PhaA and PhaB from *Ralstonia eutropha*); DSAS/CAB, co-culture of DS/CAB (DS harboring pRB1s-CAB) and AS/CAB (AS harboring pRB1s-CAB). (D) DCW, PHB, and glucose–PHB conversion at 68 h fermentation. Error bars indicate the standard deviation of duplicate cultures.

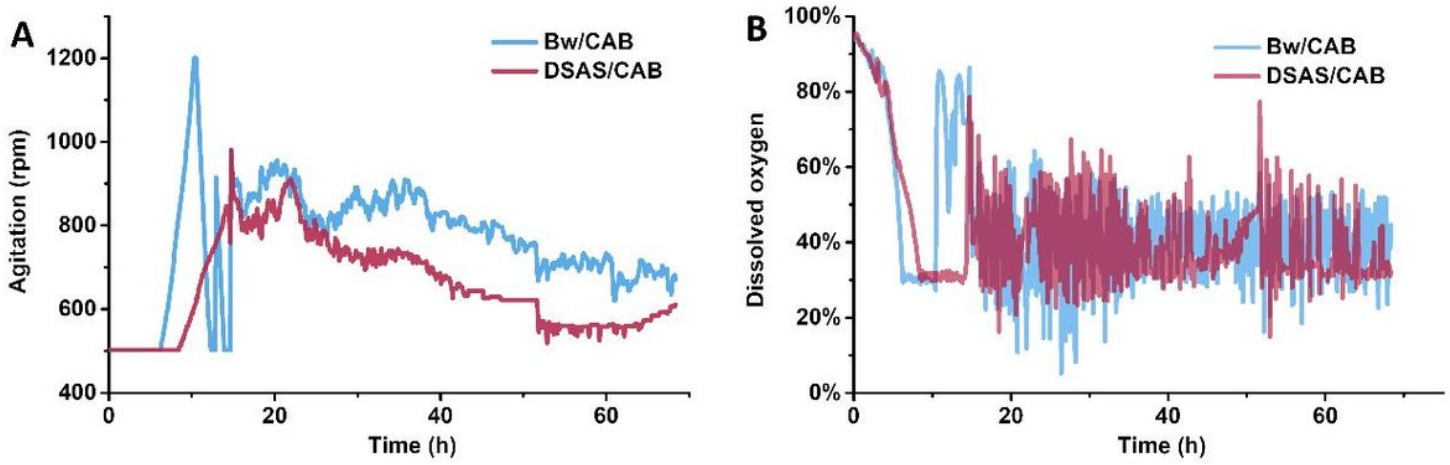

Figure 8

Overview of poly-β-hydroxybutyrate (PHB) production in 1-L fed-batch bioreactors. (A) Online agitation speed. (B) Online dissolved oxygen. Bw/CAB, BW25113 harboring pRB1s-CAB (control strain); DSAS/CAB, co-culture of DS/CAB (DS harboring pRB1s-CAB) and AS/CAB (AS harboring pRB1s-CAB).

Supplementary Files

This is a list of supplementary files associated with this preprint. Click to download.

- coculture SIChen20220308.docx

- rawdata.xlsx